

EUROPEAN ORGANIZATION FOR NUCLEAR RESEARCH  
Laboratory for Particle Physics

Divisional Report

**CERN LHC/2002-6 (VAC)**

**ION-STIMULATED GAS DESORPTION YIELDS AND THEIR DEPENDENCE  
ON THE SURFACE PREPARATION OF STAINLESS STEEL**

E. Mahner, J. Hansen, D. Küchler, M. Malabaila and M. Taborelli

Ion-induced gas desorption yields were investigated for 4.2 MeV/u lead ions incident on 316 LN stainless steel surfaces. Focussed on a possible application for the Low Energy Ion Ring (LEIR) vacuum system, the influence of surface treatments like chemical etching, electropolishing and gold-coating on the desorption yields was studied with accelerator-type vacuum chambers. The surface composition of similar prepared samples was investigated with X-ray Photoemission Spectroscopy (XPS). Desorption yields for H<sub>2</sub>, CH<sub>4</sub>, CO, Ar and CO<sub>2</sub>, which are of fundamental interest for LEIR and future accelerator applications, are reported as a function of impact angle, ion dose and charge state (+27, +53) of the lead ion beam.

CERN, Geneva, Switzerland

Presented at the Eighth European Particle Accelerator Conference (EPAC)  
3-7 June 2002 - La Villette, Paris, France

Administrative Secretariat  
LHC Division  
CERN  
CH - 1211 Geneva 23

Geneva, Switzerland  
2 July 2002

# ION-STIMULATED GAS DESORPTION YIELDS AND THEIR DEPENDENCE ON THE SURFACE PREPARATION OF STAINLESS STEEL

E. Mahner\*, J. Hansen, D. Kuchler, M. Malabaila, M. Taborelli

CERN, Geneva, Switzerland

## Abstract

Ion-induced gas desorption yields were investigated for 4.2 MeV/u lead ions incident on 316 LN stainless steel surfaces. Focussed on a possible application for the Low Energy Ion Ring (LEIR) vacuum system, the influence of surface treatments like chemical etching, electropolishing and gold-coating on the desorption yields was studied with accelerator-type vacuum chambers. The surface composition of similar prepared samples was investigated with X-ray Photoemission Spectroscopy (XPS). Desorption yields for H<sub>2</sub>, CH<sub>4</sub>, CO, Ar and CO<sub>2</sub>, which are of fundamental interest for LEIR and future accelerator applications, are reported as a function of impact angle, ion dose and charge state (+27, +53) of the lead ion beam.

## 1. INTRODUCTION

During studies performed in 1997 the static LEAR (Low Energy Antiproton Ring) vacuum pressure was about  $5 \times 10^{-12}$  Torr, but pressure bumps up to  $10^{-9}$  Torr occurred during continuous injection of about  $10^8$  ions/s [1]. A dynamic pressure increase by a factor five ( $2.5 \times 10^{-11}$  Torr) was attributed to the outgassing of equipment due to the impact of lost lead ions. Beam-induced desorption of CO molecules was found to be responsible for a large fraction of the pressure increase around the LEAR ring. More fundamental studies to understand the vacuum degradation were not done at that time. To determine the actions necessary to lower the dynamic pressure rise in LEIR, an experimental programme has been started in 2001 for measuring the molecular desorption yields of stainless steel vacuum chambers by the impact of 4.2 MeV/u lead ions with the charge state +53 or +27 [2]. In a previous study, unexpected large desorption yields of up to  $2 \times 10^4$  molecules/ion had been measured for stainless steel vacuum chambers [3]. Glow discharge treatments with Ar-O<sub>2</sub> or He-O<sub>2</sub> did not significantly reduce the desorption rates in respect to untreated stainless steel [4]. It was proposed that the bombarding lead ions might desorb molecules that are embedded deeper into the stainless steel surface than any of the various surface-cleaning methods could penetrate. Therefore, vacuum chambers have been etched, polished and coated to study the possible influence of the damaged stainless steel surface layer on the ion-induced desorption.

## 2. EXPERIMENTAL SETUP

At the CERN Heavy Ion Accelerator [5] (LINAC 3) an experiment has been installed to measure the ion-induced desorption yields for Pb<sup>53+</sup> or Pb<sup>27+</sup> at 4.2 MeV/u. An overview of the experimental set-up is shown in Figure 1.

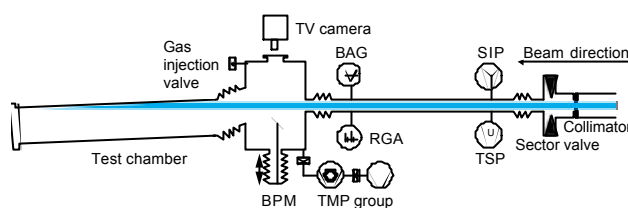


Figure 1: Ion-induced desorption experiment at the CERN Heavy Ion Accelerator .

A sector valve separates LINAC 3 from the experiment such that the test chamber may be changed without disturbing the accelerator. After the sector valve a long narrow chamber ( $\varnothing_i=35$  mm,  $\ell=1100$  mm) has been installed, which serves two purposes. First, it separates the high pressure ( $\sim 10^{-9}$  Torr) of LINAC 3 from the experiment. Second, as the test chamber is pumped through this conductance, it serves to give a known pumping speed during the experiments. A turbomolecular pumping (TMP) group is used for evacuation from atmospheric pressure, hence the test chamber is pumped via the 26.8  $\ell/s$  conductance (for H<sub>2</sub>) by a 400  $\ell/s$  sputter ion pump (SIP) and a 1200  $\ell/s$  Ti sublimation pump (TSP). Pressure measurements are made with a Bayard-Alpert gauge (BAG) and a quadrupole residual gas analyser (RGA), both calibrated. The RGA can be calibrated *in situ* via a gas injection valve. Right before the test chamber a beam position monitor (BPM), which contains an Al<sub>2</sub>O<sub>3</sub> fluorescent screen, is used for aligning the ion beam into the test chamber. A TV camera, used for beam observation and alignment, the pumping group and the gas dosing valve are mounted on the same vacuum chamber in front of the test chamber. The test chamber itself is a 1.4 m long stainless steel tube that can be tilted. The beam line parameters have been calculated, resulting in a 7.7 mm beam size at the entry and  $\sim 9.5$  mm beam size at the end of the test chamber.

\*Corresponding author. E-mail address: edgar.mahner@cern.ch

### 3. SURFACE CHARACTERIZATION

#### 3.1 Sample preparation

For surface analysis purposes platelets ( $10 \times 20 \text{ mm}^2$ ) of stainless steel 316 LN were fabricated and chemically cleaned, first by degreasing at  $50^\circ\text{C}$  with ultrasonic agitation, followed by rinsing in cold demineralised water, rinsing with alcohol and finally drying with hot air at  $80^\circ\text{C}$ . Then six samples were electropolished ( $50 \mu\text{m}$  and  $150 \mu\text{m}$ ) and chemically etched ( $50 \mu\text{m}$ ) followed by a vacuum firing ( $950^\circ\text{C}$ , 2h). Three of these platelets were then covered with  $\sim 30 \mu\text{m}$  Au deposited by galvanic coating on a  $\sim 2 \mu\text{m}$  Ni underlayer. Finally, all samples were introduced into an ultrahigh vacuum (UHV) chamber, *in situ* baked ( $300^\circ\text{C}$ , 48h) and then transferred (through air) to the surface analysis spectrometer. The air exposure was limited to less than 10 minutes.

#### 3.2 XPS surface analysis

The aim of the analysis was to compare the chemical composition of the gold-coated samples with uncoated stainless steel and to study the potential “risk” of stainless steel diffusion into the gold films during a  $300^\circ\text{C}$  bakeout. The surface contamination of three uncoated stainless steel samples, displayed in Figure 2, was independent of the initial surface treatment (as received, etched, electropolished) and mainly due to hydrocarbons adsorbed during air exposure.

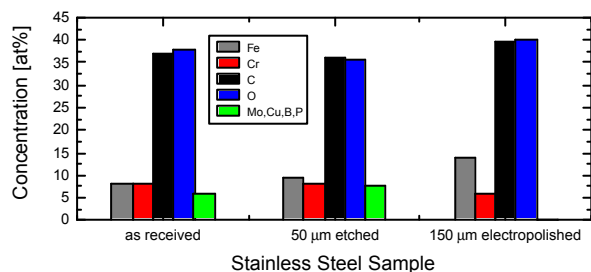


**Figure 2:** Surface composition for three different stainless steel samples after vacuum firing ( $950^\circ\text{C}$ , 2h), *in situ* bakeout ( $300^\circ\text{C}$ , 48h) and transport into the XPS system.

The chemical composition of the gold surfaces was found to be independent of the type of substrate preparation for all samples on which the Au layer had been deposited, namely:  $\sim 37\text{at}\%$  Au,  $\sim 54\text{at}\%$  C,  $\sim 8\text{at}\%$  O and  $<1\text{at}\%$  Ni+Pb. Gold exhibited the line-shape of pure metal without any binding energy shift. The main surface contaminant was carbon, which exhibited the usual line-shape of contamination adsorbed during air exposure. The line-shape of O1s showed a very wide peak ( $\sim 3 \text{ eV}$ ) indicating that several components were present, including water related species. All samples presented traces of Pb and Ni close to the instrumental detection limit ( $1\text{at}\%$ ). After moderate sputtering ( $2 \text{ keV}$ ,  $\text{Ar}^+$ ) of about  $5 \text{ nm}$ , Pb vanished; the level of Ni decreased, O and most of the C vanished.

The evolution of the surface chemical composition of a  $150 \mu\text{m}$  electropolished,  $30 \mu\text{m}$  gold-coated stainless steel sample was studied during bakeout at  $300^\circ\text{C}$  in the UHV analysis chamber. Heating removed part of the adsorbates from the surface, visible from the decrease of the C and O signals. The relative decrease was much more marked for oxygen. No surface segregation of Ni or Pb was observed during bakeout at  $300^\circ\text{C}$ . The effect of the thermal treatment as a function of temperature is shown in Figure 3 for a sample, which was successively annealed during 1h at  $200^\circ\text{C}$ ,  $300^\circ\text{C}$ , and  $380^\circ\text{C}$ .

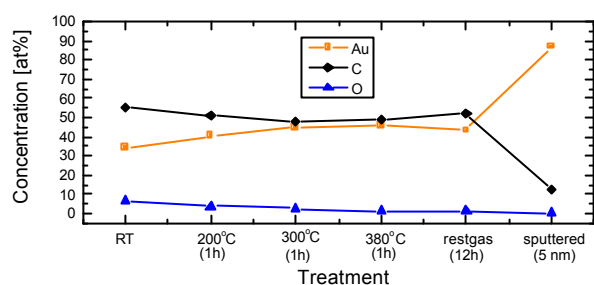


**Figure 3:** Evolution of the surface composition for a  $50 \mu\text{m}$  electropolished and  $30 \mu\text{m}$  gold-coated stainless steel sample as a function of annealing temperature, exposure to residual gas and sputtering.

A decrease of the amount of O was already observed after  $200^\circ\text{C}$  annealing, but higher temperatures were more effective in removing oxygen. Indeed, the level of O remaining after 1h at  $380^\circ\text{C}$  was lower than after 8h at  $300^\circ\text{C}$ . In contrast, the level of C could not be reduced by further increasing the temperature up to  $380^\circ\text{C}$ . Figure 3 also indicates that re-adsorption in a background pressure of  $10^{-9}$  Torr occurred, mainly constituted of  $\text{H}_2$  with CO and  $\text{H}_2\text{O}$  as minor fractions. Moderate sputtering ( $5\text{nm}$ ) strongly removed the adsorbed carbon and increased the gold signal to  $\sim 87\text{at}\%$ . We conclude that the analysed  $30 \mu\text{m}$  thick gold layers were all oxide-free, independent of the stainless steel substrate preparation. After bakeout ( $300^\circ\text{C}$ , 8h)  $\sim 49\text{at}\%$  C and  $\sim 3\text{at}\%$  O remained adsorbed on a  $30 \mu\text{m}$  thick gold layer deposited on a  $150 \mu\text{m}$  electropolished stainless steel sample.

### 4. ION-INDUCED DESORPTION RESULTS

#### 4.1 Vacuum chamber preparation

Three  $1.4 \text{ m}$  long,  $\varnothing=145 \text{ mm}$ , vacuum chambers (A, E, F) were manufactured from 316 LN stainless steel and tested at LINAC 3. The surface preparation was done in the following way:

Chamber **A**: cleaning, vacuum firing ( $950^\circ\text{C}$ , 2h) and *in situ* baking ( $300^\circ\text{C}$ , 24h).

Chamber **E**: **Test #1**: cleaning, electropolishing ( $50 \mu\text{m}$ ), vacuum firing ( $950^\circ\text{C}$ , 2h), *in situ* baking ( $300^\circ\text{C}$ , 24h).

Chamber **E**: **Test #2**: cleaning, electropolishing ( $150 \mu\text{m}$  in total), vacuum firing ( $950^\circ\text{C}$ , 2h) and *in situ* baking ( $400^\circ\text{C}$ , 24h).

Chamber **E**: **Test #3**: cleaning, gold-coating ( $\sim 30 \mu\text{m}$  on top of a  $\sim 2 \mu\text{m}$  Ni interface) of the inner surface ( $\sim 6400 \text{cm}^2$ ) and *in situ* baking ( $300^\circ\text{C}$ , 24 h).

Chamber **F**: cleaning, chemical etching ( $50 \mu\text{m}$ ), vacuum firing ( $950^\circ\text{C}$ , 2h) and *in situ* baking ( $300^\circ\text{C}$ , 24 h).

#### 4.2 Desorption yields

Effective ion-induced desorption yields  $h$  have been measured for different impact angles  $q$  with a single shot ( $560 \mu\text{s}$  long) technique [2,4] using  $\text{Pb}^{53+}$  or  $\text{Pb}^{27+}$  ions. The results are summarized in Table I. The main molecules desorbed were CO followed by  $\text{CO}_2$ , together they represented about 90-97% of the desorbed species. The  $h$ 's for  $\text{Pb}^{27+}$  were significantly lower than for  $\text{Pb}^{53+}$ . At grazing incidence ( $89.2^\circ$ ) the CO desorption of the treated stainless steel vacuum chambers (E#1, E#2, F) was reduced by a factor 3 with respect to the unpolished chamber A. The oxide-free gold surface still desorbed  $\sim 4000$  CO molecules/ $\text{Pb}^{53+}$  ion as for stainless steel (E#2). Therefore, the influence of the native stainless steel oxide layer on the ion-induced desorption remains puzzling.

	$q$	$q$	Effective Desorption Yield $h$ (molecules/ion)					Total
			$\text{H}_2$	$\text{CH}_4$	CO	Ar	$\text{CO}_2$	
<b>A</b>	+53	89.2	1570	51	13294	39	2276	17230
	+53	84.8	662	31	5382	9	1234	7318
	+53	0	861	44	7128	14	1805	9852
	+27	89.2	557	41	4357	7	613	5575
	+27	84.8	135	9	868	2	220	1234
	+27	0	92	4	816	2	222	1136
<b>E#1</b>	+53	89.2	146	21	4344	-	552	5063
<b>E#2</b>	+53	89.2	107	15	4040	-	383	4545
<b>E#3</b>	+53	89.2	370	53	4008	-	403	4834
	+53	84.8	70	12	3249	-	384	3715
	+53	0	100	21	3173	-	385	3679
	+27	89.2	312	38	250	-	81	681
	+27	84.8	15	4	213	-	29	261
	+27	0	11	3	246	-	30	290
<b>F</b>	+53	89.2	140	24	3853	-	386	4403

**Table I:** Effective desorption yields (molecules per ion) of the main desorbed molecules measured for 4.2 MeV/u lead ions incident on stainless steel vacuum chambers:

**A**: not polished, **E#1**: electropolished ( $50 \mu\text{m}$ ), **E#2**: electropolished ( $150 \mu\text{m}$ ), **E#3**: gold-coated ( $30 \mu\text{m}$ ), **F**: chemically etched ( $50 \mu\text{m}$ ). Desorption yields are tabulated as a function of the ion charge-state  $q$  and the impact angle  $q$ . Normal incidence corresponds to  $q = 0^\circ$ .

#### 4.3 Beam Cleaning

For the operation of the LEIR vacuum system the ion-induced desorption due to continuous injection of lead ions is most important to understand. Therefore, all vacuum chambers have been continuously (every 1.2 s) bombarded with  $\text{Pb}^{53+}$  ions under  $89.2^\circ$  grazing incidence for up to 145h at the maximum. The results are summarized in Figure 4. It is demonstrated that the unpolished vacuum chamber A is cleaned by continuous impact of heavy lead ions. The effective desorption yield is decreased by a factor 10 after the impact of about  $2.4 \times 10^{11}$  ions/ $\text{cm}^2$  during 15h. A factor 50 is gained after 55h

continuous  $\text{Pb}^{53+}$  bombardment. A comparison with the polished vacuum chambers (E#1, E#2, F) shows a similar beam-cleaning behaviour although the initial pressure increase, at the beginning of the beam cleaning, is significantly lower for all polished chambers. The lowest pressure increase was measured for the  $150 \mu\text{m}$  electropolished vacuum chamber coated with a  $30 \mu\text{m}$  thick gold layer. This result cannot be explained by considering the data in Table I, which do not show a correspondingly lower single-shot desorption yield for chamber E#3.

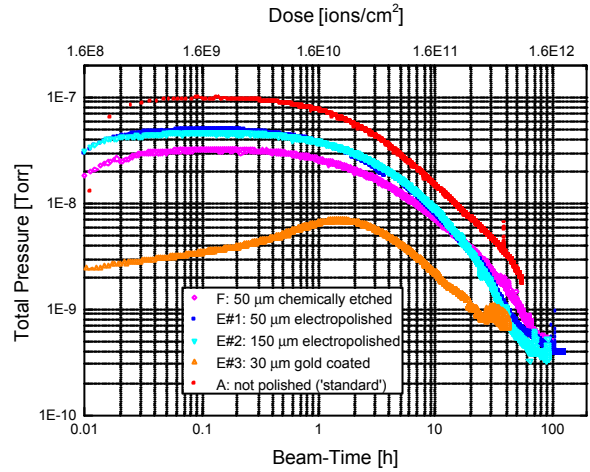


**Figure 4:** Beam-cleaning measurements for three different stainless steel vacuum chambers continuously bombarded with  $1.5 \times 10^9 \text{Pb}^{53+}$  ions under  $q = 89.2^\circ$  grazing incidence. The results obtained for a chemically etched ( $50 \mu\text{m}$ ) and an electropolished ( $50 \mu\text{m}$ ,  $150 \mu\text{m}$ ,  $30 \mu\text{m}$  gold-coating) vacuum chamber are compared with an unpolished ('standard') vacuum chamber.

## 5. CONCLUSIONS

The influence of different surface treatments (chemical etching, electropolishing, gold coating) on the heavy-ion induced molecular desorption has been shown for accelerator-type stainless steel vacuum chambers. The total effective desorption yield of polished stainless steel chambers, measured with 4.2 MeV/u  $\text{Pb}^{53+}$  ions under grazing incidence, is reduced by a factor 3-4 in comparison to an unpolished chamber. Similar desorption results were obtained for  $50 \mu\text{m}$  electropolishing ( $300^\circ\text{C}$  bakeout) and  $150 \mu\text{m}$  electropolishing ( $400^\circ\text{C}$  bakeout) of the same stainless steel vacuum chamber. The feasibility of ion-induced beam cleaning has been demonstrated. This technique will be a necessary tool to reduce the dynamic pressure of the future LEIR vacuum system.

## 6. REFERENCES

- [1] J. Bossler *et al.*, Particle Accelerators 63, 171 (1999).
- [2] J. Hansen *et al.*, CERN, LHC/VAC Note 2001-007.
- [3] M. Chanel *et al.*, Proceedings PAC 2001 (Chicago), p. 2165 (2001).
- [4] E. Mahner *et al.*, to be published.
- [5] N. Angert *et al.*, Design Report, CERN 93-01 (1993).